Phytochemical Profiling and Antioxidant Potential of Phlomoides rotata Essential Oils: Insights into Bioactive Constituents

Zheng Pan
Chongqing medical university
Chen Xie
Chongqing medical university
Jie Luo
Chongqing medical university
Wanting Zhong
Chongqing medical university
Xiaotong Yan
Chongqing medical university
Yongmei Su
Chongqing medical university
Anwar Ul Haq
Shaheed Benazir Bhutto University
Nasir Mehmood Khan
Shaheed Benazir Bhutto University
Shujaat Ahmad
Shaheed Benazir Bhutto University
Muhammad Esa
Shaheed Benazir Bhutto University
Jian Wang
wj_2000_abc@cqmu.edu.cn

Chongqing University of Chinese Medicine

Article

Keywords: Phlomoides rotata (Benth. ex Hook. f.) Mathiesen (Lamiophlomis rotata), essential oils, characteristic metabolites, norisoprenoids, biosynthesis, antioxidant activities

Posted Date: September 15th, 2025

DOI: https://doi.org/10.21203/rs.3.rs-7155967/v1

Additional Declarations: No competing interests reported.

Version of Record: A version of this preprint was published at Scientific Reports on January 11th, 2026.
See the published version at https://doi.org/10.1038/s41598-026-35657-5.

Article

Phytochemical Profiling and Antioxidant Potential of *Phlomoides rotata* Essential Oils: Insights into Bioactive Constituents

Zheng Pan [2,3], Chen Xie [2,3], Jie Luo [2,3], Wanting Zhong [2,3], Xiaotong Yan [2,3], Yongmei Su [2,3], Anwar Ul Haq [4], Nasir Mehmood Khan [5], Shujaat Ahmad [4], Muhammad Esa [4], and Jian Wang [1,2,3]*

[1] Department of Chinese Materia Medica, Chongqing University of Chinese Medicine, Chongqing 402760, China
[2] College of Traditional Chinese Medicine, Chongqing medical university, Chongqing 400016, China; 102796@cqmu.edu.cn; 2022110750@stu.cqmu.edu.cn; 2023121966@stu.cqmu.edu.cn; 2023121979@stu.cqmu.edu.cn; yxt2438249780@163.com; 101817@cqmu.edu.cn
[3] Chongqing Key Laboratory of Chinese Medicine for Prevention and Cure of Metabolic Diseases, Chongqing Medical University, Chongqing 400016, China
[4] Department of Pharmacy, Shaheed Benazir Bhutto University, Sheringal Dir (Upper) Khyber Pakhtunkhwa 18000, Pakistan; anwar@sbbu.edu.pk; shujaat@sbbu.edu.pk; esakhan5595@gmail.com
[5] Department of Agriculture, Shaheed Benazir Bhutto University, Sheringal, Upper Dir 18000, Khyber Pakhtunkhwa, Pakistan; nasir@sbbu.edu.pk
* Correspondence: wj_2000_abc@cqmu.edu.cn

The antioxidant properties and characteristic metabolites of *Phlomoides rotata* (*P. rotata*) essential oils (EOs) remain largely unexplored. To address this gap, we combined metabolomic profiling with *in vitro* antioxidant assays to systematically characterize EOs from *P. rotata*. Cryoprecipitation of EOs yielded two fractions: crystals (Crs) and crystal-free EOs (CEs). GC-MS identified 125 components (84.41-94.86%), including 94 novel reports in *P. rotata*. Dominant constituents were long-chain fatty acids (LCFAs, 42.33-75.73%) and their esters (3.44-15.21%), notably palmitic acid (14.49-63.13%), myristic acid, linoleic acid, oleic acid, and methyl palmitate. Eleven norisoprenoids, including *trans-β*-damascenone, were discovered—a fivefold increase from previously reported diversity—with their biosynthetic pathways elucidated. Eleven chemical markers were established, encompassing geraniol, linalool, *trans-β*-damascenone, hexahydrofarnesyl acetone, palmitic acid, *α*-terpineol, myristic acid, phytol, linoleic acid, oleic acid, and methyl palmitate. Palmitic acid, myristic acid, methyl palmitate, and hexahydrofarnesyl acetone showed negligible or pro-oxidative activity. Linoleic acid, oleic acid, *trans-β*-damascenone, and phytol exhibited concentration-dependent antioxidant effects. Phytol demonstrated exceptional potency, surpassing quercetin in cellular antioxidant activity at 80 μmol/L. CEs exhibited significantly stronger antioxidant capacity in both DPPH and ABTS assays compared to EOs and Crs. Palmitic acid depletion in CEs was identified as a critical factor driving enhanced antioxidant performance. This study not only establishes *P. rotata* EOs as a rich source of phytol-based antioxidants but also deciphers the dual roles of LCFAs, providing a foundation for developing natural antioxidants.

Keywords *Phlomoides rotata* (Benth. ex Hook. f.) Mathiesen (*Lamiophlomis rotata*), essential oils, characteristic metabolites, norisoprenoids, biosynthesis, antioxidant activities.

Abbreviations

EOs	essential oils
P. rotata	*Phlomoides rotata* (Benth. ex Hook. f.) Mathiesen
Crs	crystals
CEs	crystal-free EOs
FAs	fatty acids
LCFAs	long-chain FAs
CAA	cellular antioxidant activity
LRIs	linear retention indices

HPLC	High-performance liquid chromatography
DPPH	1, 1-Diphenyl-2-picrylhydrazy1
ABTS	2, 2'-azino-bis(3-ethylbenzothiazoline-6-sulfonic acid)
FBS	fetal bovine serum
DMEM	dulbecco's modified eagle medium
HBSS	Hank's Balanced Salt Solution
ABAP	2-Acetyl-4-butyramidophenol
HEPES	4-(2-Hydroxyethyl)piperazine-1-ethanesulfonic acid
ROS	reactive oxygen species
CCK	Cell counting kit
GC-FID	gas chromatography-flame ionization detector
GC-MS	gas chromatography-mass spectrometry
FFAP	free fatty acid phase
NIST	National Institute of Standards and Technology
TICs	total ion chromatograms
RT	retention time
PCA	principal component analysis
PLS-DA	partial least squares discriminant analysis
VIP	variable importance in projection
FRAP	ferric reducing/antioxidant power
RSA	radical scavenging activity
HepG2	Human Hepatoma-derived G cell line 2
EDTA	Ethylene Diamine Tetraacetic Acid
PBS	Phosphate Buffer Saline
ANOVA	analysis of variance
DMSO	dimethyl sulfoxide
PVDF	polyvinylidene fluoride
DCFH-DA	2', 7'-dichlorodihydrofluorescein diacetate
Hepes	4-(2-hydroxyethyl)-1-piperazineethanesulfonic acid
MEP/DoXP	2-C-Methyl-D-erythritol 4-phosphate/1-Deoxy-D-xylulose 5-phosphate

Phlomoides rotata (Benth. ex Hook. f.) Mathiesen (*P. rotata*), also known as *Lamiophlomis rotata* (Benth.) Kudô, is a medicinal herb called "Duyiwei" (*Lamiophlomis herba*). It is found in high altitudes in China[1-4]. Traditionally, the root, rhizome, or the entire herb are used for medicinal purposes[5,6]. Its underground parts are known for promoting blood circulation, eliminating stasis, reducing swelling, and providing analgesic effects. The above-ground parts are used for treating grasserie, fractures, injuries from falls, osteomyelitis, gunshot injuries, and edema pain[2,5-7]. In clinical practice, *P. rotata* is typically used directly without any prior processing, mainly for pain relief[6].

Due to the low content of volatile chemicals, the focus has primarily been on its involatile compounds. So far, at least 223 chemical constituents have been isolated and identified, including iridoids, flavonoids, phenylethanoid glycosides, polysaccharides, organic acids, volatile oils, and others[6,7]. The main compounds found are iridoid glycosides, which are responsible for the analgesic effect[6,7] and serve as chemical markers to assess the quality of Duyiwei[7]. Norisoprenoids (also called apocarotenoids)[8] have been largely overlooked. Only two compounds of C13-norisoprenoids, 5*β*, 6*α*-dihydroxy-3*β*-(*β*-D-glucopyranosyloxy)-7-megastigmen-9-one[6,7,9] and 3*β*-hydroxy-5*α*, 6*α*-epoxy-7-megastigmen-9-one[6,10], and one compound of C18-norisoprenoids, hexahydrofarnesyl acetone, were reported[11]. As of now, only one study has reported the chemicals in EOs extracted from *P. rotata* using steam distillation[12]. Another study has reported the lipophilic composition in the CH_2Cl_2 extracted part[11]. In total, 81 compounds are reported, whcih can be seen in supplemental Table 1[11,12]. However, some identifications are still debatable, such as oleic acid, ethyl linoleate, and cyclohexenylacetic acid, taking

into consideration the values of linear retention indices (LRIs) and the mass spectra[11,12]. Only three compounds, myristic acid, palmitic acid, and linoleic acid, were detected in both studies[11,12]. The main compounds found in terms of content are fatty acids (FAs), especially long-chain fatty acids (LCFAs) such as palmitic acid, myristic acid, oleic acid, and linoleic acid[11,12]. Furthermore, some bound volatiles such as *α*-terpineol-8-O-*β*-D-glucopyranoside and (2Z)-2, 6-dimethyl-6-hydroxyocta-2, 7-dienyl-O-*β*-D-glucopyranoside have been found[7].

There have been limited studies on the in-depth biological effects of volatile oils from *P. rotata*[7]. Oxidative stress, recognized as a critical mediator in rheumatoid arthritis pathogenesis, oncogenic transformation, and diabetic complications[13,14], underscores the therapeutic imperative for novel antioxidants. However, the reactive oxygen species (ROS)-scavenging capacity of *P. rotata* EOs remains unexplored. Our earlier work on *P. rotata* established the anti-hepatic fibrosis efficacy of polyphenolic glycosides and diabetic wound-healing acceleration of iridoid glycosides[15-17]. The foundation now drives the current exploration of volatile antioxidants. This pioneering investigation elucidates the antioxidant activities of chemical markers in *P. rotata* EOs through gas chromatography-mass spectrometry (GC-MS) metabolomics and ROS scavenging assays, establishing phytochemical baselines for developing novel natural antioxidants in pharmaceutical applications.

Materials and Methods

Plant Materials, Reagents and Chemicals

The aboveground portion of *P. rotata* was collected from BianBa (28°21'31.6"N 91°15'48.3"E), LeiWuQi (31°12'24.4"N 96°34'56.6"E) and NaQu (31°29'18.4"N 92°00'03.6"E) counties of Tibet during the flowering period in August 2018 and was dried in the shade. The voucher specimen were numbered as L8, L9, and L10, which corresponded to the same sample numbers used in a previous research study[15]. The voucher specimen were identified by professor Yi Zhang (Chengdu University of Traditional Chinese Medicine, Chengdu, China) and using Internal transcribed spacer 2 deoxyribonucleic acid barcodes, as described in the previous study[15]. These voucher samples were deposited in the College of Ethnic Medicine at Chengdu University of Traditional Chinese Medicine (Chengdu, China), and the Chongqing Academy of Chinese Materia Medica (Chongqing, China). Experimental research and field studies on plants (either cultivated or wild), including the collection of plant material, were conducted in accordance with relevant institutional, national, and international guidelines and legislation.

The following reagents and chemicals were used: *n*-hexane (High-performance liquid chromatography (HPLC) grade), linalool (98%+), *p*-cymene (99%+), *α*-terpineol (98%+), and nonane (98%), which were produced by Adamas Reagent Company Limited; *d*-limonene (96%) produced by Acros Organics, the United States of America; *γ*-terpinene (97%) produced by Wako Pure Chemical Industries, Limited, Japan; palmitic acid produced by CATO Research Chemicals Incorporated; *n*-Alkanes standard solution of C_{10}-C_{25} produced by Dr. Ehrenstorfer Incorporated, Germany; *n*-octacosane (99%) produced by Aldrich; 1, 1-Diphenyl-2-picrylhydrazyl (DPPH), 2, 2'-azino-bis(3-ethylbenzothiazoline-6-sulfonic acid) (ABTS) powder, and potassium persulfate ($K_2S_2O_8$). All these reagents and chemicals were supplied by Shanghai Titan Scientific Company Limited, China. MeOH, used for preparative liquid phase, was sourced from Shanghai Lingfeng Chemical Reagent Company Limited and supplied by Yonghua Chemical Company Limited; MeOH (HPLC grade), fetal bovine serum (FBS), dulbecco's modified eagle medium (DMEM), high glucose, double antibodies: penicillin-streptomycin solution, Hank's Balanced Salt Solution (HBSS), 2-Acetyl-4-butyramidophenol (ABAP), and 4-(2-Hydroxyethyl)piperazine-1-ethanesulfonic acid (HEPES), produced by Adamas-beta, were supplied by Shanghai Titan Scientific Company Limited, China; ROS assay kit, Cell counting kit (CCK)-8 test kits were purchased from Beyotime Biotechnology, China.

Extraction and separation

Weighed powders of L8, L9, and L10 (315 g each) were placed in separate round-bottomed 5L flasks. Pure water (3150 mL, 10 times volume compared with weight) was added to each flask. The mixtures were soaked for 0.5 hours at 40 °C. The EOs were extracted three times from each powder using hydrodistillation with a Clevenger-type apparatus. Each extraction lasted for 5 hours. *n*-Hexane was employed as the collecting solvent. The collected EOs, which appeared as light yellow, were treated with anhydrous Na_2SO_4 to eliminate any residual water.

To evaluate crystallization, the EOs of L8, L9, and L10 were stored at different temperatures: 4 °C, -4 °C, and -80 °C. Crystals (Crs) were obtained either at 4 °C or -4 °C. However, at -80 °C, the crystal-free EOs (CEs) of all three samples were in a solid state. Each sample was stored in separate screw-capped vials at 4 °C.

The identification and quantitation of chemicals in the EOs, Crs, and CEs

Sample preparation

There are three sets of samples for L8, L9, and L10: EOs, Crs, and CEs. Specifically, there are nine samples: EO8, EO9, EO10, Cr8, Cr9, Cr10, CE8, CE9, and CE10. These samples were prepared according to the following procedure. For the detection acquired by gas chromatography-flame ionization detector (GC-FID) using a DB-5 column and GC-MS using a DB-5 column, the samples were diluted in the ratio of $Volume_{sample}$:$Volume_{n\text{-hexane}}$ 1:1000 (0.1%). For the detection acquired by GC-MS using a free fatty acid phase (FFAP) column, the samples were diluted at a ratio of $Volume_{sample}$:$Volume_{n\text{-hexane}}$ 1:250 (0.4%).

Chromatograms obtained from GC analyses

GC-FID analyses were conducted using a GC-2010 instrument from Shimadzu, Japan, equipped with a DB-5 column (30 m × 0.25 mm inner diameter, 0.25 μm film thickness). The following parameters were used: the oven temperature was programmed from 60 °C with a 3-minute hold, and then ramped up to 250 °C at a rate of 2.5 °C per minute. The final temperature was held for 2 minutes. Nitrogen was used as the carrier gas, with a constant flow rate of 1.7 mL per minute. Both the injector and the detector were maintained at 250 °C. The sample was split in a ratio of 5:1. Each sample was injected once with a volume of 1 μL.

GC-MS analyses were performed using a GCMS-TQ8040 instrument from Shimadzu, Japan. Separately, either a DB-5 column or a FFAP column (30 m × 0.32 mm × 0.5 μm) was used. For the DB-5 column: The oven temperature was programmed from 60 °C with a 3-minute hold, and then ramped up to 280 °C at a rate of 2.5 °C per minute. The final temperature was held for 2 minutes. Helium was used as the carrier gas, with a constant flow rate of 1 mL per minute. The sample was split in a ratio of 100:1. A solvent delay of 3.0 minutes was implemented. The injector was maintained at 250 °C, while the ion-source and interface were maintained at 200 °C and 250 °C, respectively. Mass spectra were acquired at 70 eV with a scan rate of 3.9 scans per second, covering the mass range from m/z 25 to 450 amu. Each sample was injected once with 1 μL. For FFAP column: The oven temperature was programmed from 60 °C with a 3-minute hold, and then ramped up to 230 °C at a rate of 2.5 °C per minute. The final temperature was held for 2 minutes. The rest of the parameters (carrier gas, splitting ratio, solvent delay, temperature of injector, ion-source, and interface, mass spectra, injection times, and injection volume) remained the same as for the DB-5 column.

Identification

Either a National Institute of Standards and Technology (NIST) 14 or a NIST 17 MS database was utilized. Initially, the peaks in the total ion chromatograms (TICs) were identified using probability-based matching. However, due to the presence of overlapped and embedded peaks in the TICs, the identification results may sometimes be inaccurate. In such cases, characteristic ion peaks were selected and compared with the NIST 14 or 17 database, as well as the mass spectra of known standards. By employing a combination of probability-based matching and comparing characteristic ion peaks, the compound identification process becomes more reliable, particularly when dealing with overlapping peaks. This approach enhances the overall accuracy and confidence in the identification results.

The LRIs values were calculated using the equation (1) proposed by Van Den Dool and Kratz[18]. In equation (1), "t_n" and "t_{n+1}" represent the retention time (RT) of the *n*-Alkanes (C_{10}-C_{25}, C_{28}, and the detected C_{26}-C_{27}, C_{29}) with the corresponding number ("n") of carbons. "t_x" represents the RT of the detected compound x (t_x), where "$t_n \leq t_x \leq t_{n+1}$". Furthermore, the RT of *n*-triacontane (t_{30}) was deduced by analyzing the TICs obtained through GC-MS using a FFAP column.

$$LRI = 100n + 100\left[\frac{t_x - t_n}{t_{n+1} - t_n}\right] \quad (1)$$

The $LRIs^b$ were gotten by a DB-5 column, and $LRIs^d$ were gotten by a FFAP column in this experiment. $LRIs^a$ were obtained by a semi-standard apolar column, while $LRIs^c$ were obtained by a polar column, which are recorded in the NIST 17 library or the database[19,20]. The $LRIs^b$ and $LRIs^d$ were compared with the $LRIs^a$ and $LRIs^c$, respectively.

Quantification

The overlapped peaks in the TICs were deconvoluted into individual peaks based on the characteristic ion peaks of the corresponding matching compound. The relative area percentage of each compound was calculated using peak area normalization.

Principal component analysis (PCA) and partial least squares discriminant analysis (PLS-DA)

Rigorous preprocessing was applied to the data in Table 1. Initially, missing values were inspected and addressed using mean imputation. To minimize noise interference, compounds with significant missing

data—such as *trans*-calamenene, *trans*-*β*-ocimene, isoterpinolene, *cis*-11-eicosenoic acid methyl ester, and 4-acetyl-1-methylcyclohexene—were excluded, resulting in a dataset with 120 quantified compounds. All data were standardized to ensure comparability across variables. Multivariate analyses were conducted using the R package ropls (version 1.32.0) to construct PCA and PLS-DA models. Visualization of sample score plots, x-variable loadings, and variable importance in projection (VIP) scores was accomplished with ggplot2 (version 3.5.1) to facilitate comprehensive interpretability. A 10-fold cross-validation was employed to assess the stability and predictive capacity of the models, helping to prevent overfitting. Additionally, a permutation test with 2000 iterations was conducted to evaluate the statistical significance of the models. VIP scores calculated from the PLS-DA model were used to quantify the contribution of each x-variable to class discrimination. Higher VIP values indicate greater importance in distinguishing and explaining model outcomes. The threshold for VIP was set to ≥1.2 to identify potential characteristic markers[21].

Analyses of metabolic pathways

The metabolic pathways of the chemicals were analyzed by MetaboAnalyst 6.0, a web-based tool (https://www.metaboanalyst.ca/), as well as the Kyoto Encyclopedia of Genes and Genomes system (https://www.kegg.jp/kegg/). Specifically, the results were visualized in "Figure 3", which was generated using MetaboAnalyst 6.0.

Antioxidant activities of EOs, Crs, CEs, and eight chemical markers

The antioxidant capacities of nine samples, EO8, EO9, EO10, Cr8, Cr9, Cr10, CE8, CE9, and CE10, were tested by DPPH, ABTS, and ferric reducing/antioxidant power (FRAP) assays, respectively. Additionally, eight chemical markers including palmitic acid, myristic acid, oleic acid, linoleic acid, methyl palmitate, phytol, hexahydrofarnesyl acetone, and *trans*-*β*-damascenone, were included in the analyses. Quercetin were used as reference compounds.

Samples preparation

All the subjects were diluted in MeOH. Since there was a limited amount of volatile oils available, only three low concentrations, namely 50, 80, and 110 μg/mL, were set up for the nine samples. The phytol and *trans*-*β*-damascenone were diluted to specific concentrations of 6.25, 12.5, 25, 50, and 100 mmol/L, respectively. The oleic acid and linoleic acid were diluted to specific concentrations of 100, 200, 500, 1000, and 2000 mmol/L, respectively. The palmitic acid and myristic acid were diluted to specific concentrations of 50, 100, 200, 500, and 1000 mmol/L, respectively. The methyl palmitate and hexahydrofarnesyl acetone were diluted to specific concentrations of 50, 100, 200, 500, and 1000 mol/L, respectively. The quercetin was diluted to 2.5, 5, 10, 20, and 50 μmol/L, respectively.

DPPH assay

A slight modification was made to the experimental procedure[22]. The samples, each 100 μL, at various concentrations were added to individual wells of a 96-well microplate. Subsequently, 100 μL of DPPH solution (100 μmol/L) also diluted with MeOH was added to each well. The microplate was then incubated in darkness at room temperature for 30 minutes. After the incubation period, the absorbance of the reaction mixture was measured at 517 nm using a microplate reader. Each sample was analyzed in triplicate, and MeOH was used as the blank control. The radical scavenging activity (RSA) was calculated using the following equation:

$$\mathrm{RSA}(\%) = \left[\frac{A_{\mathrm{Blank}} - A_{\mathrm{Sample}}}{A_{\mathrm{Blank}}}\right] \times 100\% \quad (2)$$

Where A_{Blank} is the absorbance of the blank control (MeOH) and A_{Sample} is the absorbance of the reaction mixture. The RSA value indicates the percentage of DPPH radical scavenged by the sample, with higher values indicating stronger antioxidant activities.

ABTS assay

The methodology from prior research[23] was refined through a minor adjustment to enhance precision. To prepare the ABTS radical cation ($ABTS^{\bullet+}$) solution, 5 mL of a 7 mM aqueous ABTS solution was reacted with 88 μL of a 140 mM $K_2S_2O_8$ aqueous solution (resulting in a final concentration of 2.45 mM for $K_2S_2O_8$). The reaction mixture was kept in darkness at room temperature for 16 hours. Subsequently, the radical cation solution was diluted with MeOH, typically around 30-50 times, until its absorbance reached a value of 0.7±0.02 at 734 nm. For each sample, 100 μL was added to 100 μL of the ABTS radical solution. The mixture was thoroughly mixed at room temperature for 6 minutes. Following the incubation period, the absorbance at 734 nm was measured using a microplate reader. The calculation method for RSA was consistent with that used in the DPPH assay.

FRAP assay

A slight modification was made to the method described in a previously published study[24]. For each sample, 100 μL was added to 100 μL of the FRAP working solution. The FRAP working solution was composed of acetic acid buffer (0.3 mol/L), 2, 4, 6-Tris (2-pyridyl)-1, 3, 5-triazine solution (10 mmol·L^{-1}), and $FeCl_3$ (20 mmol·L^{-1}) solution, with a volume ratio of 10:1:1. The sample and the FRAP working solution were thoroughly mixed and then placed in darkness at 37 °C for a 30-minute incubation period. After incubation, the absorbance of the mixture at 593 nm was immediately measured using a microplate reader. The increase in absorbance at this wavelength indicates the reduction capacity of the samples and provides information on their antioxidant potential.

To establish the calibration curve, Fe (II) aqueous solutions (0.01-0.2 mmol/L) were mixed with the FRAP reagent at a 1:1 volume ration (0.1 mL each). In this measuring system, the total antioxidant capacity was determined in terms of Fe (II) equivalents. The concentration of $FeSO_4$ (mmol·L^{-1}) was calculated based on the absorbance value obtained from the standard curve after the reaction, which was referred to as the FRAP value. A higher FRAP value indicates a stronger antioxidant capacity.

Cell culture

Human Hepatoma-derived G cell line 2 (HepG2) cells were cultured in DMEM containing 10% (v/v) FBS and 1% (v/v) penicillin-streptomycin at 37 °C with 5% CO_2. Routine subculturing was performed every 3-4 days using 0.25% trypsin-Ethylene Diamine Tetraacetic Acid (EDTA) solution when cells reached approximately 80% confluence.

Cell viability

HepG2 cells were seeded in 96-well plates at a density of 2×10^4 cells/well. After 24-hour adherence, monolayers were gently washed with Phosphate Buffer Saline (PBS) and exposed to treatments (1-500 μmol/L in complete medium) for 24 hours. After PBS washing, cells were incubated with 10% (v/v) CCK-8 solution prepared in serum-free medium for 1 hour at 37 °C under 5% CO. Cell viability was quantified by absorbance at 450 nm. The non-cytotoxic concentration - defined as the highest dose showing no significant difference ($P > 0.05$) compared to vehicle controls in one-way analysis of variance (ANOVA) - was selected for downstream experiments. Standard solutions were prepared by dissolving in dimethyl sulfoxide (DMSO), final concentration ≤ 0.1% (v/v), sterile-filtered through 0.22 μm polyvinylidene fluoride (PVDF) membranes, and stored at -20 °C in sterile microcentrifuge tubes. Vehicle controls contained equivalent DMSO concentrations.

Cellular antioxidant activity (CAA)

The CAA was quantified following the established protocol[25]. HepG2 cells were plated in 96-well plates (6×10^4 cells/well) and cultured for 24 h. After PBS washing, cells were incubated with extracts (in 100 μL treatment medium containing 5 μM 2', 7'-dichlorodihydrofluorescein diacetate (DCFH-DA) for 1 h. Following PBS removal, oxidative stress was induced using 600 μM ABAP in HBSS/4-(2-hydroxyethyl)-1-piperazineethanesulfonic acid (Hepes) (10 mM) buffer. Real-time fluorescence kinetics (excitation λ 485 nm/emission λ 538 nm) were recorded every 5 min for 60 min at 37 °C using a microplate reader. CAA values were calculated by equation (3).

$$CAA\ unit = 1 - \left(\frac{\int SA}{\int CA}\right) \quad (3)$$

$\int$ SA is the integrated area under the sample fluorescence versus time curve and $\int$ CA is the integrated area from the control curve.

Results and discussion

Extraction and separation

From *P. rotata* with Voucher No. L8, L9, and L10, a total of 0.29 g, 0.26 g, and 0.19 g of light yellow EOs were obtained, corresponding to 418, 405, and 238 μL, respectively. The yields were calculated as 0.13%, 0.13%, and 0.08%, respectively, based on the ratio of the volume of the EOs (in mL) to the weight of the *P. rotata* (in g) (mL/g). The average yield of 0.11% is in close agreement with the previously reported yield of 0.1%[12].

The densities of the EOs were measured as 0.69, 0.64, and 0.8, respectively. These EOs have a fresh and elegant smell. The Crs were separated from the EOs at temperatures of 4 °C or -4 °C, and the CEs were subsequently obtained by removing the Crs.

The EOs extracted from *P. rotata* exhibit certain similarities to the EOs extracted from *Malva sylvestris* L.[26], *Cirsium japonicum* var. *ussurience* Kitamura, *Ixeris dentate*, and *I. stolonifera*[27,28] also

with low extraction rates. This similarity is attributed to the high content of palmitic acid and hexahydrofarnesyl acetone in these extracts[26-28].

Chemicals in the EOs of *P. rotata*

In total, 125 compounds were identified and quantified. Among them, 31 were previously documented in literatures[11,12], while 94 constituents represent novel findings from *P. rotata*, as summarized in Table 1 and illustrated in Figure 1.

Table 1. The compounds in the EOs of *P. rotata* (%)

Codes	Compounds	CAS#	LRIs[a]	LRIs[b]	LRIs[c]	LRIs[d]	EO8	Cr8	CE8	EO9	Cr9	CE9	EO10	Cr10	CE10
CA1	Acetic acid	64-19-7	610	-	1449	1449	0	0.02	0.09	0	0.02	0.01	0.03	0.03	0.05
CA2	Propanoic acid	79-09-4	700	700	1535	1535	0	0.01	0.09	0	0.02	0.02	0	0.01	0.03
CA3	Senecic acid	541-47-9	953	951	1782	1787	0	0.01	0.03	0	0.02	0.02	0.01	0.02	0.04
CA4	Hexanoic acid	142-62-1	990	971	1846	1838	0	0.11	0.26	0	0.17	0.38	0.09	0.17	0.40
CA5	Caprylic acid	124-07-2	1180	1169	2060	2053	0.06	0.09	0.20	0	0.07	0.13	0.11	0.08	0.17
CA6	Nonanoic acid	112-05-0	1273	1269	2171	2156	0.06	0.13	0.34	0	0.08	0.24	0.16	0.20	0.36
CA7	*n*-Decanoic acid	334-48-5	1373	1369	2276	2262	0.16	0.20	0.39	0.40	0.35	0.70	0.31	0.32	0.59
CA8	Undecanoic acid	112-37-8	1475	1475	2400	2367	0.06	0.09	0.12	0	0.21	0.41	0.11	0.15	0.29
CA9	Dodecanoic acid	143-07-7	1568	1564	2497	2474	0.75	0.87	1.57	0.86	1.24	2.05	0.88	1.12	1.40
CA10	Tridecanoic acid	638-53-9	1666	1662	2617	2579	0.11	0.25	0.45	0.20	0.27	0.47	0.27	0.21	0.40
CA11	Myristic acid	544-63-8	1768	1760	2694	2685	3.62	5.29	5.22	2.89	4.18	4.58	3.33	5.13	4.95
CA12	Pentadecanoic acid	1002-84-2	1867	1862	2822	2790	0.43	0.65	0.57	0.63	0.44	0.61	0.33	0.61	0.88
CA13	9*E*-Hexadecenoic acid	2091-29-4	1942	1939	2954	2935	0.84	0.78	2.19	0	0.28	0.51	0.36	0.26	0.59
CA14	Palmitoleic acid	373-49-9	1951	1956	2926	2926	1.62	1.02	3.53	1.04	0.86	1.11	0.61	0.83	1.21
CA15	Palmitic acid	57-10-3	1968	1960	2931	2894	46.28	59.15	14.49	43.73	63.13	31.20	40.47	54.81	38.58
CA16	Linoleic acid	60-33-3	2133	2129	3164	2884	7.61	1.00	7.94	5.26	0.85	1.20	4.35	0.54	0.00
CA17	Oleic acid	112-80-1	2141	2137	3173	2770	2.65	2.77	5.72	2.56	2.91	8.55	3.14	3.73	0.00
CA18	Stearic acid	57-11-4	2172	2163	3136	2700	2.22	3.83	0.64	0	1.58	1.69	0.65	3.34	0.00
	Carboxylic acids (18)						66.48	76.26	43.84	57.57	76.67	53.88	55.23	71.57	49.94
	FAs (15)						66.48	76.22	43.64	57.57	76.62	53.82	55.19	71.51	49.82
	LCFAs (10)						66.14	75.61	42.33	57.17	75.73	51.96	54.42	70.58	48.02
E1	Lavender lactone	1073-11-6	1043	1034	1684	1656	0	0.01	0.02	0	0.02	0.03	0	0.03	0.04
E2	Benzoic acid, 4-methyl-, methyl ester	99-75-2	1215	1217	1740	1733	0	0.02	0.05	0	0.06	0.19	0.09	0.08	0.09
E3	Geranyl formate	105-86-2	1300	1297	1695	1705	0.01	0.01	0.21	0	0.02	0.03	0.04	0	0.02
E4	Nonanoic acid, 9-oxo-, methyl ester	1931-63-1	1436	1437	-	2041	0.02	0.05	0.21	0	0.09	0.16	0.13	0.11	0.20
E5	Methyl laurate	111-82-0	1526	1523	1804	1802	0	0.01	0.05	0	0.02	0.09	0.04	0.04	0.07
E6	2(4H)-Benzofuranone, 5,6,7,7a-tetrahydro-4,4,7a-trimethyl-	15356-74-8	1538	1540	2327	2283	0	tr	0.08	0	0.03	0.04	0.01	0.05	0.01
E7	Methyl tetradecanoate	124-10-7	1725	1724	2005	2008	0.08	0.14	0.22	0.17	0.12	0.30	0.22	0.20	0.41
E8	Tetradecanoic acid, 12-methyl-, methyl ester	5129-66-8	1788	1785	-	2077	0	0.02	0.04	0	0	0.05	0	0.03	0.02
E9	Methyl pentadecanoate	7132-64-1	1820	1816	2108	2111	0	0.02	0.02	0	0.03	0.07	0.02	0.04	0.06

E10	Methyl palmitoleate	1120-25-8	1898	1901	2240	2239	0.07	0.10	0.23	0.23	0.13	0.28	0.14	0.12	0.22
E11	Methyl hexadec-9-enoate	10030-74-7	1904	1908	2238	2231	0	0.02	0.04	0	0.03	0.05	0.02	0.04	0.06
E12	Methyl palmitate	112-39-0	1926	1924	2208	2214	1.39	1.53	3.40	3.07	2.77	6.09	3.69	3.99	7.33
E13	Ethyl palmitate	628-97-7	1993	1992	2251	2253	0.04	0.08	0.21	0.08	0.09	0.20	0.11	0.13	0.27
E14	Methyl margarate	1731-92-6	2028	2025	2309	2318	0.02	0.08	0.17	0	0.07	0.19	0.11	0.13	0.24
E15	Methyl oleate	112-62-9	2091	2091	2434	2439	0.79	0.67	1.75	1.73	1.82	4.12	2.30	2.12	3.90
E16	Methyl linoleate	112-63-0	2092	2098	2482	2485	1.89	0.29	2.32	4.26	0.55	0.84	3.99	0.46	0.71
E17	Methyl linolenate	301-00-8	2098	2100	2571	2552	1.76	0.03	0.95	2.72	0.05	0.07	3.23	0.03	0.03
E18	Methyl elaidate	1937-62-8	2110	2104	2445	2446	0.02	0.08	0.16	0	0.13	0.27	0.10	0.11	0.25
E19	Methyl stearate	112-61-8	2128	2123	2418	2420	0.22	0.30	0.56	0.18	0.27	0.74	0.43	0.45	0.81
E20	Phytol acetate	10236-16-5	2218[19]	2218	-	2512	0.09	0.16	0.48	0	0.10	0.23	0.20	0.26	0.32
E21	*cis*-11-Eicosenoic acid, methyl ester	2390-09-2	2306		-	2645	0	0	0	0	0	0	0	0	0.12
E22	Methyl 5,6-octadecadienoate	-	-		-	2515	0.14	0.07	0.29	0.50	0.63	1.44	0.34	0.29	0.71
	Esters (22)						6.53	3.68	11.44	12.95	7.00	15.44	15.21	8.67	15.85
	Esters of FAs (17)						6.43	3.49	10.63	12.95	6.79	14.96	14.88	8.28	15.41
	Esters of LCFAs (16)						6.41	3.44	10.42	12.95	6.70	14.80	14.76	8.17	15.21
N1	Sulcatone	110-93-0	986	980	1338	1340	0	tr	0.03	0	0.01	tr	0.04	0.01	0.01
	C8-norisoprenoids (1)						0	tr	0.03	0	0.01	tr	0.04	0.01	0.01
N2	Dehydro-ar-ionene	30364-38-6	1354	1354	1732	1729	0.05	0	0.09	0	0	0.02	0.14	0.02	0.04
N3	*trans*-*β*-Damascenone	23726-93-4	1386	1379	1823	1808	0.34	tr	0.16	0.46	0.02	0.03	0.43	0.02	0.04
N4	Hexahydropseudoionone	1604-34-8	1408	1406	1660	1685	0	0.01	0.02	0	0.01	0.02	0.05	0.01	0.03
N5	2-Buten-1-one, 1-(2,6,6-trimethyl-1-cyclohexen-1-yl)-	35044-68-9	1417	1415	1830	1801	0.01	0.01	0.02	0	tr	0.01	0.03	0.03	0.03
N6	*α*-Ionone	127-41-3	1426	1429	1840	1834	0	0	0	0	0	tr	0	tr	tr
N7	*trans*-Geranylacetone	3796-70-1	1453	1450	1859	1849	0.11	0.05	0.22	0.14	0.04	0.09	0.25	0.07	0.13
N8	*β*-Ionon-5,6-epoxide	23267-57-4	1473	1472	1962	1969	0	0.02	0.04	0	0.02	0.06	0.01	0.06	0.14
N9	*trans*-*β*-Ionone	79-77-6	1486	1486	1940	1920	0.26	0.01	0.13	0.25	0.01	0.03	0.56	0.04	0.04
	C13-norisoprenoids (8)						0.77	0.10	0.69	0.85	0.11	0.28	1.47	0.26	0.45
N10	Hexahydrofarnesyl acetone	502-69-2	1844	1843	2131	2119	1.90	2.50	5.11	2.06	2.12	5.18	2.91	3.45	6.23
N11	Farnesyl acetone	1117-52-8	1919	1915	2384	2362	0.62	0.09	0.80	0.38	0.09	0.13	0.89	0.11	0.20
	C18-norisoprenoids (2)						2.52	2.58	5.91	2.45	2.20	5.31	3.79	3.56	6.43
	Norisoprenoids (11)						3.29	2.68	6.63	3.30	2.32	5.59	5.31	3.83	6.90
MA1	*cis*-Linalool oxide	5989-33-3	1074	1066	1445	1441	0.11	0.42	0.80	0.21	0.58	1.28	0.20	0.69	1.25
MA2	*trans*-Linalool oxide	34995-77-2	1086	1084	1452	1468	0.07	0.36	0.57	0.07	0.52	1.10	0.15	0.59	1.00
MA3	Linalool	78-70-6	1099	1099	1547	1552	2.23	0.66	3.30	3.98	1.07	1.85	3.65	1.23	1.98
MA4	Hotrienol	29957-43-5	1107	1107	1613	1612	0	0	0	0.74	0	0	0.38	0	0

MA5	*β*-Terpineol	138-87-4	1153	1139	1627	1625	0	0.01	0.01	0	0	0	0	0	tr
MA6	*cis*-Linalool 3,7-oxide	14009-71-3	1174	1169	1751	1759	0	0.04	0.04	0	0.07	0.16	0	0.09	0.18
MA7	*trans*-Linalool 3,7-oxide	39028-58-5	1173	1173	1739	1732	0	0.06	0.08	0	0.07	0.13	0.01	0.06	0.16
MA8	Terpinen-4-ol	562-74-3	1177	1174	1602	1595	0.11	0.03	0.13	0.16	0.04	0.05	0.10	0.04	0.04
MA9	*m*-Cymen-8-ol	5208-37-7	1180	1176	1845	1842	0	0.02	0.04	0	0.03	0.06	0.03	0.02	0.03
MA10	*α*-Terpineol	98-55-5	1189	1185	1697	1690	2.66	1.04	3.88	3.88	1.21	1.96	3.17	1.21	1.57
MA11	3,7-Octadiene-2,6-diol, 2,6-dimethyl-	13741-21-4	1190	1190	1945	1944	0	0.06	0.17	0	0.06	0.12	0.05	0.07	0.12
MA12	Citronellol	106-22-9	1228	1222	1765	1766	0	0	0.02	0.17	0.03	0.05	0.04	0.02	0.04
MA13	*cis*-Geraniol	106-25-2	1228	1224	1797	1797	0.16	tr	0.09	0.19	0.02	0.03	0.17	0.02	0.02
MA14	2-Hydroxycineol	18679-48-6	1228	-	1845	1846	0	0.13	0.07	0	0.11	0.27	0.01	0.25	0.24
MA15	Geraniol	106-24-1	1255	1252	1847	1846	0.51	0.09	0.23	0.44	0.11	0.13	0.37	0.00	0.10
	Monoterpenoid alcohols (15)						5.86	2.93	9.43	9.83	3.92	7.18	8.33	4.30	6.75
DA1	Isophytol	505-32-8	1948	1947	2296	2290	0.30	0.37	0.83	0.22	0.22	0.53	0.36	0.38	0.77
DA2	Phytol	150-86-7	2114	2110	2622	2607	5.41	1.41	5.72	2.11	0.65	1.09	4.15	1.26	1.81
	Diterpenoid alcohols (2)						5.71	1.77	6.55	2.33	0.87	1.63	4.51	1.64	2.58
Al1	Tridecane	629-50-5	1300	1300	1300	1300	0	0	0.01	0	0	0	tr	0	0.01
Al2	**Farnesane**	3891-98-3	1366	1371	1354	1354	0	0.02	0.03	0.11	0	0.02	0.02	0.01	0.02
Al3	Tetradecane	629-59-4	1400	1400	1400	1400	0.04	tr	0.05	0	0	0.01	0.04	tr	0.02
Al4	Pentadecane	629-62-9	1500	1500	1500	1500	0.04	0.03	0.10	0	0.01	0.05	0.06	0.02	0.07
Al5	Hexadecane	544-76-3	1600	1600	1600	1600	0.05	0.05	0.12	0	0.04	0.12	0.06	0.05	0.16
Al6	Hexadecane, 2-methyl-	1560-92-5	1664	1660	1658	1660	0.01	0.03	0.04	0	0.01	0.03	0	0.02	0.02
Al7	Pentadecane, 2,6,10,14-tetramethyl-	1921-70-6	1687	1686	1670	1669	0.04	0.06	0.07	0	0.04	0.10	0.08	0.08	0.18
Al8	Heptadecane	629-78-7	1700	1700	1700	1700	0.10	0.10	0.24	0.11	0.09	0.26	0.13	0.13	0.30
Al9	Phytan	638-36-8	1792	1792	-	1775	0.11	0.06	0.15	0	0.04	0.10	0.08	0.08	0.15
Al10	Octadecane	593-45-3	1800	1800	1800	1800	0.01	0.04	0.10	0.05	0.02	0.10	0.05	0.05	0.14
Al11	Nonadecane	629-92-5	1900	1900	1900	1900	0.03	0.03	0.07	0	0.02	0.03	0.01	0.02	0.05
Al12	Eicosane	112-95-8	2000	2000	2000	2000	0.03	0.04	0.08	0	0.02	0.07	0	0.03	0.08
Al13	Heneicosane	629-94-7	2100	2100	2100	2100	0.02	0.03	0.06	0	0.02	0.08	0.05	0.06	0.11
Al14	Docosane	629-97-0	2200	2200	2200	2200	0.02	0.06	0.09	0	0.06	0.15	0.07	0.09	0.17
Al15	Tricosane	638-67-5	2300	2300	2300	2300	0.17	0.19	0.42	0.28	0.22	0.53	0.22	0.20	0.40
Al16	Tetracosane	646-31-1	2400	2400	2400	2400	0.14	0.13	0.26	0	0.12	0.33	0.08	0.10	0.18
Al17	Pentacosane	629-99-2	2500	2500	2500	2500	0.19	0.25	0.46	0.40	0.19	0.59	0.15	0.15	0.37
Al18	Hexacosane	630-01-3	2600	2600	2600	2600	0.17	0.10	0.28	0.18	0.06	0.13	0.24	0.06	0.15
Al19	Heptacosane	593-49-7	2700	2700	2700	2700	0.20	0.65	0.42	0.63	0.98	1.31	0.25	1.17	1.02
Al20	Octacosane	630-02-4	2800	2800	2800	2800	0.24	0.28	0.45	0	0.13	0.41	0.25	0.23	0.38
Al21	Nonacosane	630-03-5	2900	2900	2900	2900	0.47	1.21	0.15	0	0.64	0.55	0	0.55	0
	Alkanes (21)						2.08	3.37	3.65	1.76	2.73	4.98	1.84	3.10	3.96
MAH1	*p*-Menth-1-en-9-al	29548-14-9	1229	-	1620	1606	0.15	0	0.05	0	0	0	0.14	0.01	0.02

MAH 2	*α*-Citral	141-27-5	1270	1266	1732	1722	0.02	0.01	0.10	0	0.02	0.04	0.07	0.03	0.04
	Monoterpenoid aldehydes (2)						0.17	0.01	0.15	0	0.02	0.04	0.20	0.04	0.06
MP1	2,3-Dehydro-1,8-cineole	92760-25-3	991	993	1195	1193	0	0	0.02	0	tr	0.01	0	0.01	0.01
MP2	(-)-*cis*-Rose oxide	3033-23-6	1106[19]	1107	1337[20]	1351	0	0	0.02	0.14	0.06	0.09	0.09	0.02	0.06
MP3	(-)-*trans*-Rose oxide	5258-11-7	1127	1125	1367	1365	0	0	0.01	0	0.03	0.06	0.03	0.02	0.02
MP4	Nerol oxide	1786-08-9	1153	1154	1469	1469	0	0	0	0.07	0	0	0.03	0	0
	Monoterpenoid pyrans (4)						0	0	0.06	0.21	0.10	0.16	0.15	0.05	0.09
Se1	*β*-Caryophyllene	87-44-5	1419	1415	1595	1583	0.08	0.08	0.07	0.23	0.03	0.05	0.12	0.02	0.05
Se2	α-Humulene	6753-98-6	1454	1449	1667	1658	0	0.12	0.01	0	0	0.01	0	0	tr
Se3	*trans*-Calamenene	73209-42-4	1529	1523	1826	1818	0	0	0.05	0	0	0	0	0	0
	Sesquiterpenes (3)						0.08	0.21	0.13	0.23	0.03	0.05	0.12	0.02	0.05
AA1	1-Pentanol	71-41-0	765	764	1250	1250	0	0.01	0.03	0	0.02	0.02	0	0.01	0.02
AA2	2-Hexanol	626-93-7	801	800	1220	1221	0	0.01	0.04	0.07	0.01	0.02	0.05	0.02	0.02
AA3	3-Hexanol	623-37-0	797	800	1198	1198	0.02	tr	0.04	0.05	0.01	0.02	0.05	0.01	0.02
AA4	1-Octen-3-ol	3391-86-4	980	972	1450	1454	0.39	0.14	0.65	1.56	0.59	1.02	1.45	0.61	1.00
AA5	3-Octanol	589-98-0	994	989	1393	1397	0.01	tr	0.02	0.16	0.06	0.09	0.05	0.03	0.04
AA6	1-Undecanol	112-42-5	1371	1369	1852	1864	0	0.01	0.03	0	0.02	0.04	0.02	0.02	0.01
AA7	1-Hexadecanol	36653-82-4	1880	1877	2382	2375	0.05	0.06	0.12	0	0.02	0.04	0.04	0.03	0.05
AA8	1-Heptadecanol	1454-85-9	1984	1980	2475	2466	0	0	0.08	0	0	0.04	0	0	0.04
	Aliphatic alcohols (8)						0.46	0.23	1.00	1.84	0.73	1.29	1.67	0.74	1.22
SA1	Spathulenol	6750-60-3	1576	1572	2136	2102	tr	tr	0.02	0	0.01	0.02	0.01	0.01	0.03
SA2	Cedrol	77-53-2	1598	1600	2116	2086	0.06	0.06	0.13	0	0.09	0.21	0.08	0.07	0.14
	Sesquiterpenoid alcohols (2)						0.06	0.06	0.14	0	0.09	0.23	0.09	0.09	0.16
Me1	*β*-Pinene	127-91-3	979	972	1112	1114	0.04	0.01	0	0	0	0.01	0	0	0.01
Me2	*β*-Myrcene	123-35-3	991	989	1161	1167	0.05	0.04	0	0	0	0.01	0	0	0
Me3	*p*-Cymene	99-87-6	1025	1021	1272	1272	0.15	0.26	0.07	0.12	0.02	0.04	0.10	0.02	0.04
Me4	Limonene	138-86-3	1030	1026	1200	1203	3.04	2.81	0.64	1.41	0.19	0.48	0.74	0.12	0.28
Me5	*trans*-*β*-Ocimene	3779-61-1	1049	1044	1250	1255	0	0.02	0	0	0	0	0	0	0
Me6	*γ*-Terpinene	99-85-4	1060	1054	1246	1247	0.16	0.16	0	0	0	tr	0.01	0	0.01
Me7	Isoterpinolene	586-63-0	1086	1084	1286	1287	0	0.02	0	0	0	0	0	0	0
	Monoterpenes (7)						3.44	3.31	0.72	1.53	0.20	0.53	0.85	0.14	0.34
De1	Neophytadiene	504-96-1	1837	1838	1922	1926	0.09	0.03	0.09	0	0	0.02	0.06	0.03	0.04
	Diterpenes (1)						0.09	0.03	0.09	0	0	0.02	0.06	0.03	0.04
O1	3-Hexanone	589-38-8	784	782	1053		0.01	0.01	0.02	0	0.01	0.01	0.03	0.01	0.01
O2	2-Hexanone	591-78-6	790	792	1083		0.03	tr	0.02	0	0.01	0.01	0.03	0.01	0.01
O3	Hexanal	66-25-1	800	800	1083		0	0.07	0.23	0	0.08	0.14	0.03	0.07	0.12
O4	1-Octen-3-one	4312-99-6	979	971	1300	1305	0	0.01	0.04	0.02	0.02	0.04	0.06	0.03	0.04
O5	4-Acetyl-1-methylcyclohexene	6090-09-1	1137	1136	1568	1544	0	0	0.02	0	0	0.01	0	0	0
O6	2-Nonenal, (*E*)-	18829-56-6	1162	1160	1534	1530	0.03	0	0.05	0	0	0.01	0.06	0.01	0.01
O7	1-Tetradecene	1120-36-1	1392	1389	1443	1445	0.01	0	0.06	0	0	0.01	0.02	0	0
O8	Cetene	629-73-2	1592	1591	1648	1647	0.03	0.14	0.07	0	0.02	0.04	0.04	0.02	0.03

O9	2-Pentadecanone	2345-28-0	1698	1695	2019	2014	0.02	0.02	0.05	0	0.02	0.05	0.04	0.03	0.04
	Others (9)						0.13	0.25	0.55	0.02	0.16	0.33	0.31	0.17	0.27
	Total oxygenated compounds (90)						88.61	87.75	79.57	88.05	91.86	85.70	90.81	91.05	83.75
	Total (125)						94.39	94.81	84.41	91.58	94.86	91.39	93.88	94.40	88.23

Notes: The percentage was calculated by the peak areas gotten from the TICs obtained by GC-MS using a FFAP column. "tr" indicates trace quantities (<0.005% and >0). The chemicals denoted with red are reported already[11,12].

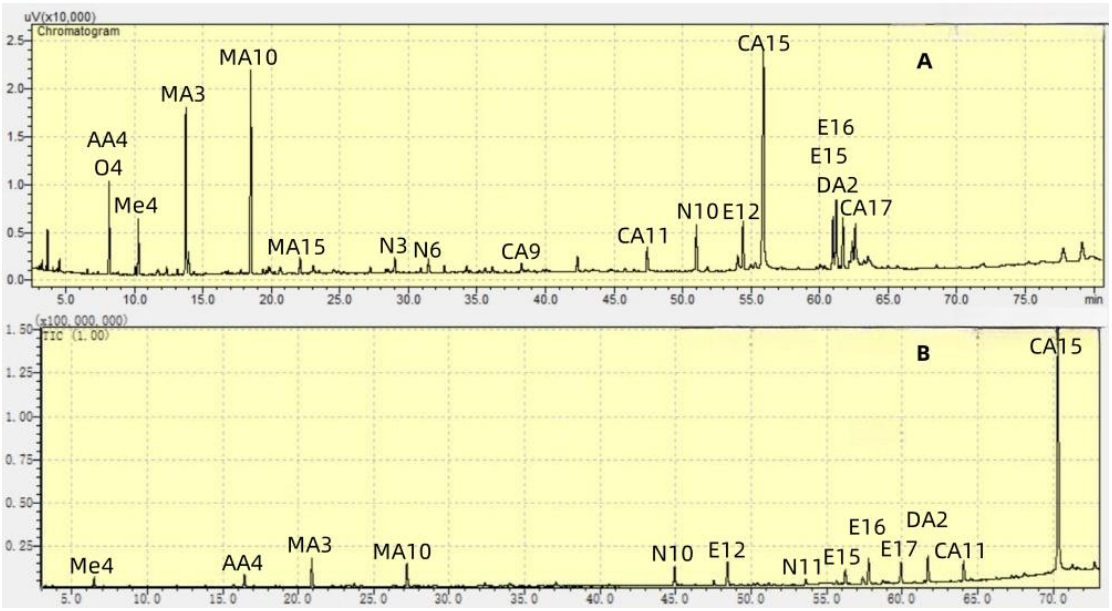

Figure 1. The chromatograms of EO10. Each denoted compound is assigned the corresponding code as listed in Table 1. "**A**" and "**B**" was obtained by GC-FID using a DB-5 column and GC-MS using a FFAP column, respectively.

These compounds belong to various classes, mainly including FAs, esters of FAs, norisoprenoids and monoterpenoid alcohols. The high sample dilution and elevated split ratio resulted in limited detectable peaks in the TICs acquired with a DB-5 column. In such scenario, just nine compounds were identified: hexanal, 1-octen-3-ol, limonene, linalool, α-terpineol, hexahydrofarnesyl acetone, methyl palmitate, palmitic acid, and oleic acid. Notably, limonene, α-terpineol, and palmitic acid exhibited significantly higher relative abundances compared to other constituents.

The mass spectra of compounds CA16, CA17, and CA18 closely resemble those of linoleic acid, oleic acid, and stearic acid, respectively. However, their LRIs[d] values of 2884, 2770, and 2700 are significantly different from the corresponding LRIs[c] values recorded in NIST 17 database, which are 3164, 3173, and 3136, respectively. Considering the MS oven temperature program of FFAP, the maximum calculated LRIs[d] value is 2984. This suggests that chemicals with LRIs[c] values higher than 2984, such as linoleic acid, oleic acid, and stearic acid, will not be eluted under the employed analytical conditions and will be eluted in the subsequent chromatogram, which can significantly alter their LRIs[d] values. The absence of these compounds in the first detected sample of EO8 supports this hypothesis. Consequently, the compounds CA15, CA16, and CA17 are still identified as linoleic acid, oleic acid, and stearic acid, respectively, which were also reported previously[11,12].

The EOs, Crs, and CEs primarily consist of FAs, particularly LCFAs. Palmitic acid (14.49-63.13%) stands out as the most prominent FAs, which aligns with the reported findings[11,12]. The Crs contain a relatively higher content of palmitic acid compared to that of the EOs and CEs. Additionally, myristic acid, oleic acid, and linoleic acid are also significant, as previously reported[11,12]. The 9-hexadecenoic acid reported previously[12] is most likely corresponding to the 9*E*-hexadecenoic acid detected in this study, based on their LRIs values. Regarding the ester of FAs, the major compounds are methyl palmitate, methyl oleate, methyl linoleate, and methyl linolenate.

Among the monoterpenoid alcohols, *α*-terpineol and linalool is relatively prominent. Geraniol as the biosynthetic precursor of iridoid is first identified in *P. rotata*.

The relatively high levels of *α*-terpineol, linalool, and limonene, may be attributed to the introduction of EOs derived from Nanfengmiju (*Citrus kinokuni* Hort. ex Tanaka) peels, which were analyzed simultaneously[29]. These monoterpenoids are characteristic constituents of *Citrus* EOs[29].

Regarding percentages, seven compounds are highlighted, namely palmitic acid, myristic acid, linoleic acid, oleic acid, methyl palmitate, hexahydrofarnesyl acetone, and phytol.

As for norisoprenoids, only hexahydrofarnesyl acetone was detected formerly[11]. The content of C13-norisoprenoids is relatively less, and its content in the Crs is relatively less compared to that in the corresponding EOs or CEs.

Despite their low abundance, C13-norisoprenoids exert disproportionate organoleptic influence in EOs due to potent flavor characteristics[30]. Notably, *trans-β*-damascenone emerges as a key natural aroma compound within this class[31], exhibiting a distinctively sweet, fruity, and warm flavor[32]. Its exceptionally low odor thresholds (0.002 μg/L in water or 5 μg/L in 25% alcohol)[30-32] enable significant aromatic contributions even at trace concentrations. Therefore, *trans-β*-damascenone is a critical determinant of the unique aroma profile in *P. rotata* EOs.

trans-β-Damascenone is primarily formed through the degradation of precursors when heated under acidic conditions[30]. In this study, it is likely that *trans-β*-damascenone was produced from the progenitors during the process of hydro-distillation[33]. Similar mechanisms have been observed for the generation of other volatile C13-norisoprenoids[30,33]. The compound 5*β*, 6*α*-dihydroxy-3*β*-(*β*-D-glucopyranosyloxy)-7-megastigmen-9-one, previously isolated from *P. rotata*[9], can act as a potential precursor for the synthesis of the eight types of C13-norisoprenoids (Fig. 2).

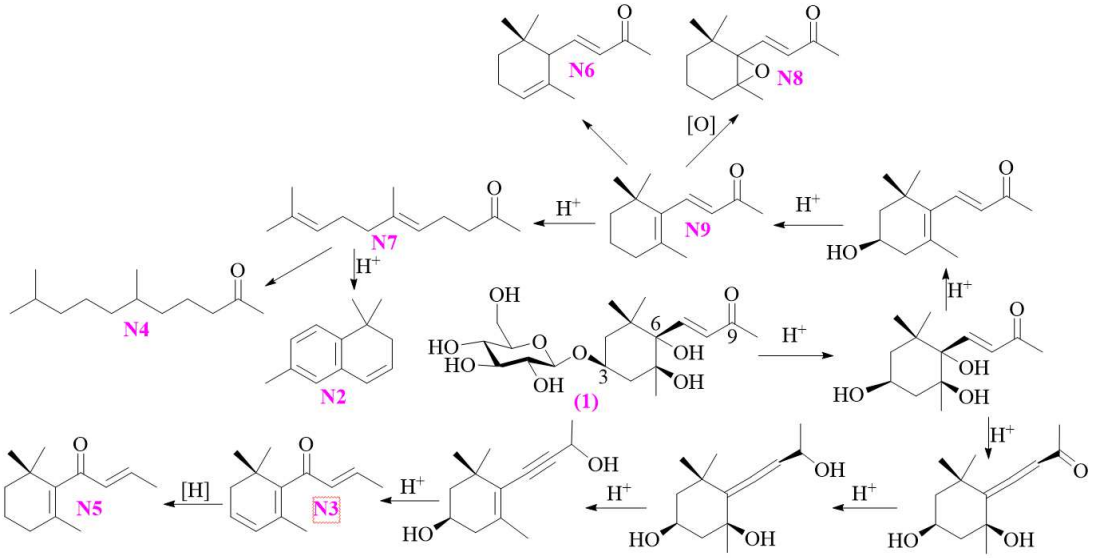

Figure 2. The hypothetical transformation process from 5*β*, 6*α*-dihydroxy-3*β*-(*β*-D-glucopyranosyloxy)-7-megastigmen-9-one **(1)** to eight different types of C13-norisoprenoids. The arrows represent the enzymatic steps involved.

PCA and PLS-DA of the samples and metabolites

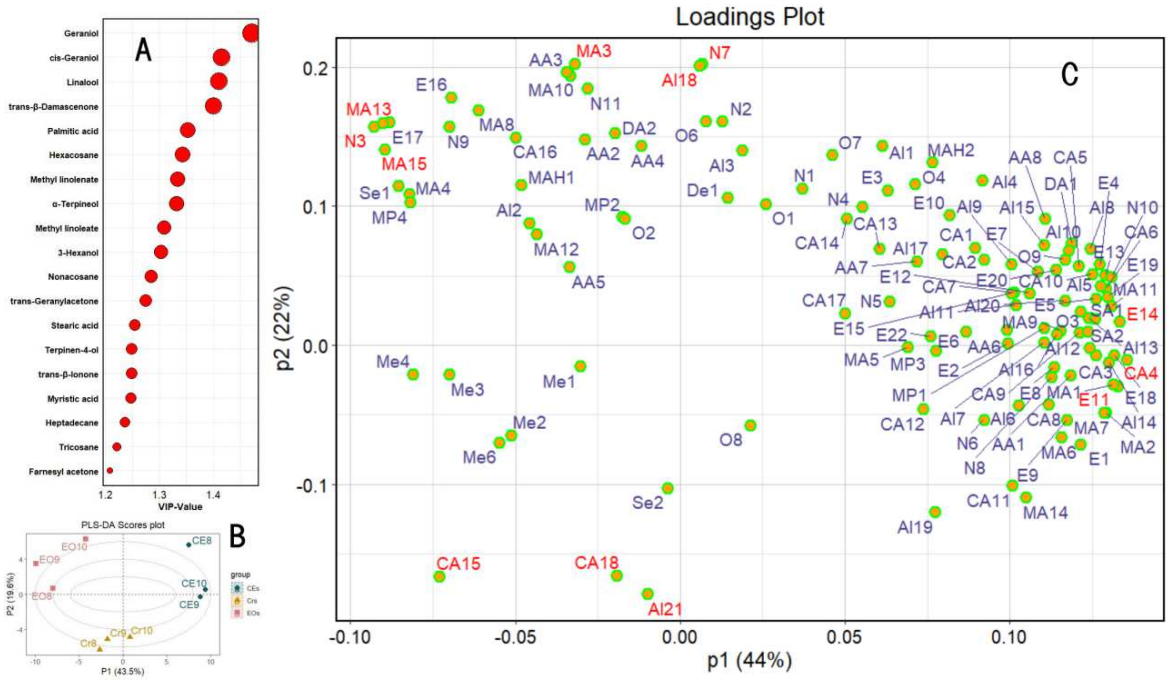

Figure 3. A Nineteen compounds were selected based on a VIP value of 1.2 or higher. **B** The PLS-DA scores plot. The nine samples were divided into three categories. **C** The loading plot of each constituent in PLS-DA. The red-highlighted compounds demonstrate the most substantial contributions to principal components 1 and 2, including E14 (methyl margarate), CA4 (hexanoic acid), E11 (methyl hexadec-9-enoate), CA18 (stearic acid), CA15 (palmitic acid), MA13 (*cis*-geraniol), MA15 (geraniol), MA3 (linalool), N3 (*trans*-*β*-damascenone), N7 (*trans*-geranylacetone), Al18 (hexacosane), and Al21 (nonacosane).

In Fig. 3B, CE8 is positioned farther apart. The chemical similarity among plant samples L8, L9, and L10 correlates with their geographical proximity, suggesting that shared environmental conditions may influence their metabolic profiles.

Analyses of metabolic pathways

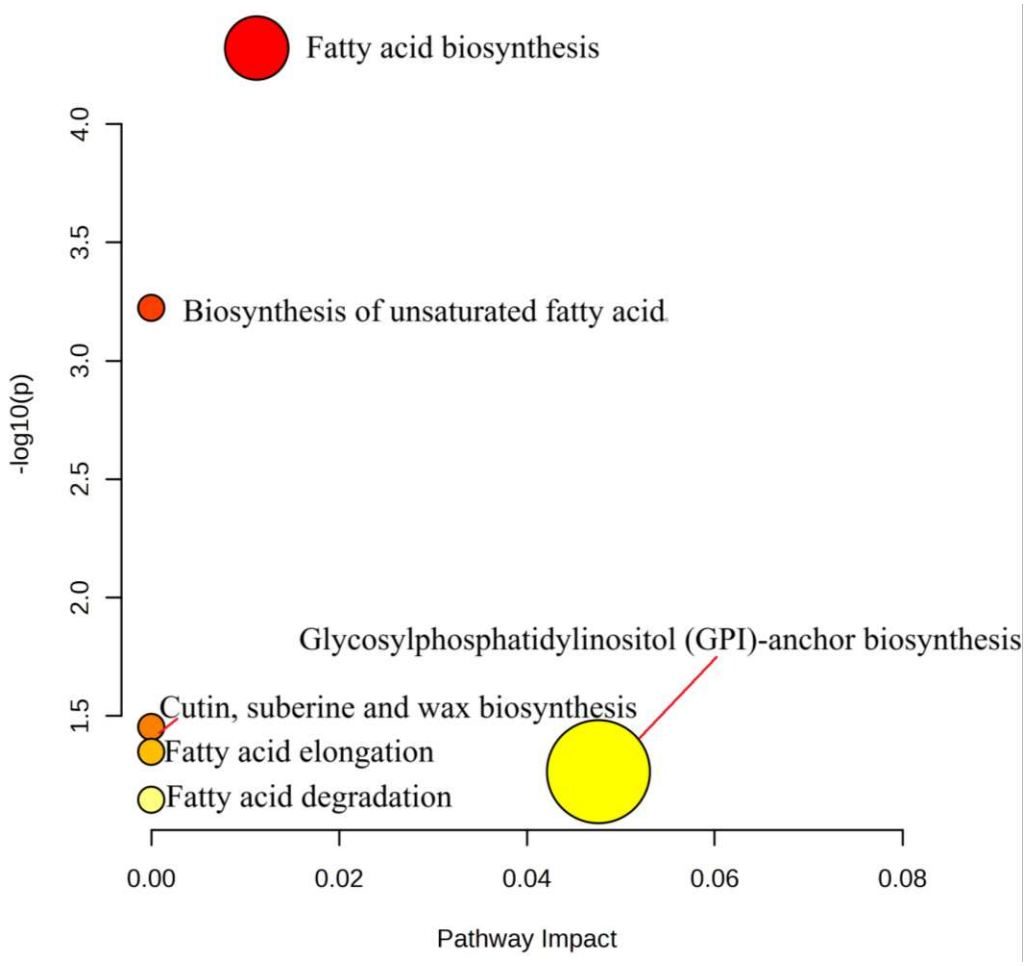

Figure 4. The main metabolic pathways. The color of the nodes is rendered based on the *p*-value (significance). The red circles usually represent a smaller *p*-value (high significance), indicating that the metabolite is differentially expressed or significantly enriched in the pathway. The size of the circles reflects the topological importance of the metabolite in the pathway, which is calculated based on topological parameters in the pathway analysis, such as node degree, betweenness centrality, *etc.*. The larger the circle, the stronger the connectivity of the metabolite in the pathway network, the more crucial its function, and the higher its overall impact (Impact Score) on the pathway. The color (significance) and size (importance) need to be analyzed in combination: nodes with high significance (red) and large circles are usually the key differentially expressed metabolites in the pathway and require special attention.

The volatiles in plants are mainly biosynthesized by carbohydrates, FAs and amino acids[8,34]. The biosynthesis of diverse volatile compounds originates from only a few primary metabolic pathways, including the shikimate pathway, 2-C-Methyl-D-erythritol 4-phosphate/1-Deoxy-D-xylulose 5-phosphate (MEP/DoXP) pathway, mevalonate pathway, and lipoxygenase pathway. Terpenoid volatiles are synthesized by the cytosolic mevalonic acid and the plastidial MEP/DoXP pathways, the former giving rise to sesquiterpenes, irregular terpenes, and the latter to monoterpenes, diterpenes and volatile carotenoid derivatives (apocarotenoids)[34]. Norisoprenoids are the derivatives of carotenoids[8]. For example, sulcatone, *trans*-geranylacetone, farnesyl acetone are derived from phytoene; *α*-ionone is derived from *δ*-carotene; and *β*-ionone is derived from *β*-carotene[8].

The screening of chemical markers and their biosynthesis

Through integrative analysis of the 19 metabolites (geraniol, *cis*-geraniol, linalool, *trans*-*β*-damascenone, palmitic acid, hexacosane, methyl linolenate, *α*-terpineol, methyl linoleate, 3-hexanol, nonacosane, *trans*-geranylacetone, stearic acid, terpinen-4-ol, *trans*-*β*-ionone, myristic acid, heptadecane, tricosane, farnesyl acetone) (Fig. 3A), 12 compounds (methyl margarate, hexanoic acid, methyl hexadec-9-enoate, stearic acid, palmitic acid, *cis*-geraniol, geraniol, linalool, *trans*-*β*-damascenone, *trans*-geranylacetone, hexacosane, nonacosane) (Fig. 3C), the nine constituents (hexanal, 1-octen-3-ol, limonene, linalool, *α*-terpineol, hexahydrofarnesyl acetone, methyl palmitate, palmitic acid, and oleic acid) detected by GC-

MS using a DB-5 column, and the ten relative abundant compounds (palmitic acid, myristic acid, methyl palmitate, oleic acid, hexahydrofarnesyl acetone, linoleic acid, phytol, α-terpineol, linalool, methyl oleate), a total of 11 compounds were validated as robust chemical markers: geraniol, linalool, *trans*-β-damascenone, hexahydrofarnesyl acetone, palmitic acid, α-terpineol, myristic acid, phytol, linoleic acid, oleic acid, and methyl palmitate.

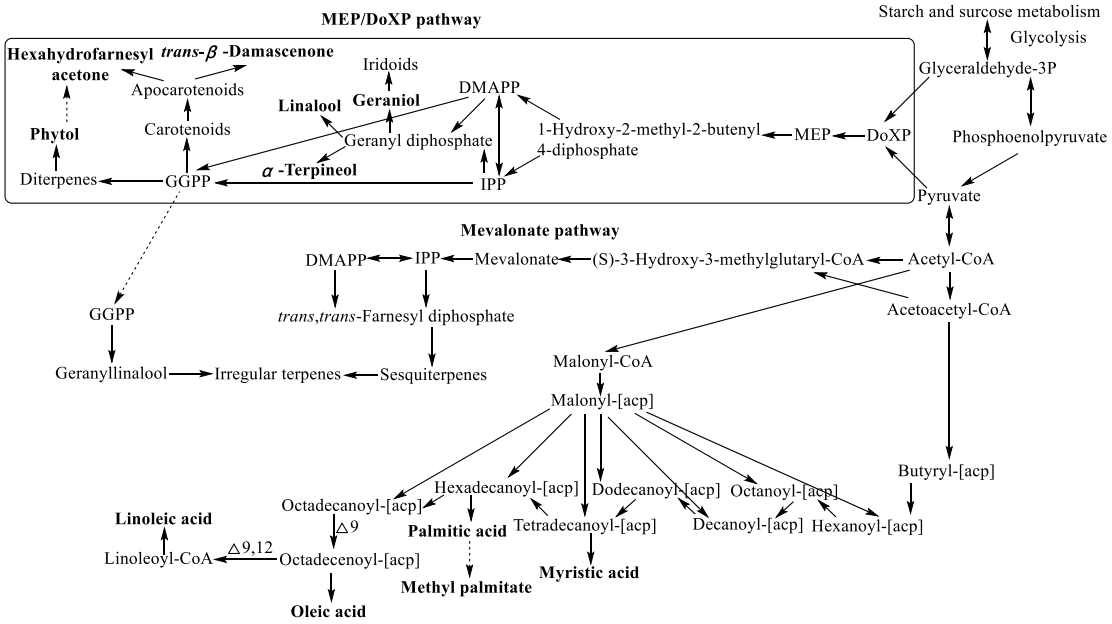

Figure 5. The biosynthesis of chemical markers. Solid arrows represent established biosynthetic steps, whereas dashed line arrows indicate the transformation is hypothetical. DMAPP, IPP, GGPP, and acp correspond to dimethylallyl diphosphate, isopentenyl diphosphate, geranylgeranyl diphosphate, and acyl-carrier protein, respectively.

Antioxidant activities of EOs, Crs, CEs, and eight chemical markers such as palmitic acid, *trans*-β-damascenone, myristic acid, hexahydrofarnesyl acetone, phytol, linoleic acid, oleic acid, and methyl palmitate

In the DPPH and ABTS assay (Fig. 6), CE10 exhibits the highest RSA value among the nine samples. Palmitic acid, myristic acid, methyl palmitate, and hexahydrofarnesyl acetone demonstrate pro-oxidant activities.

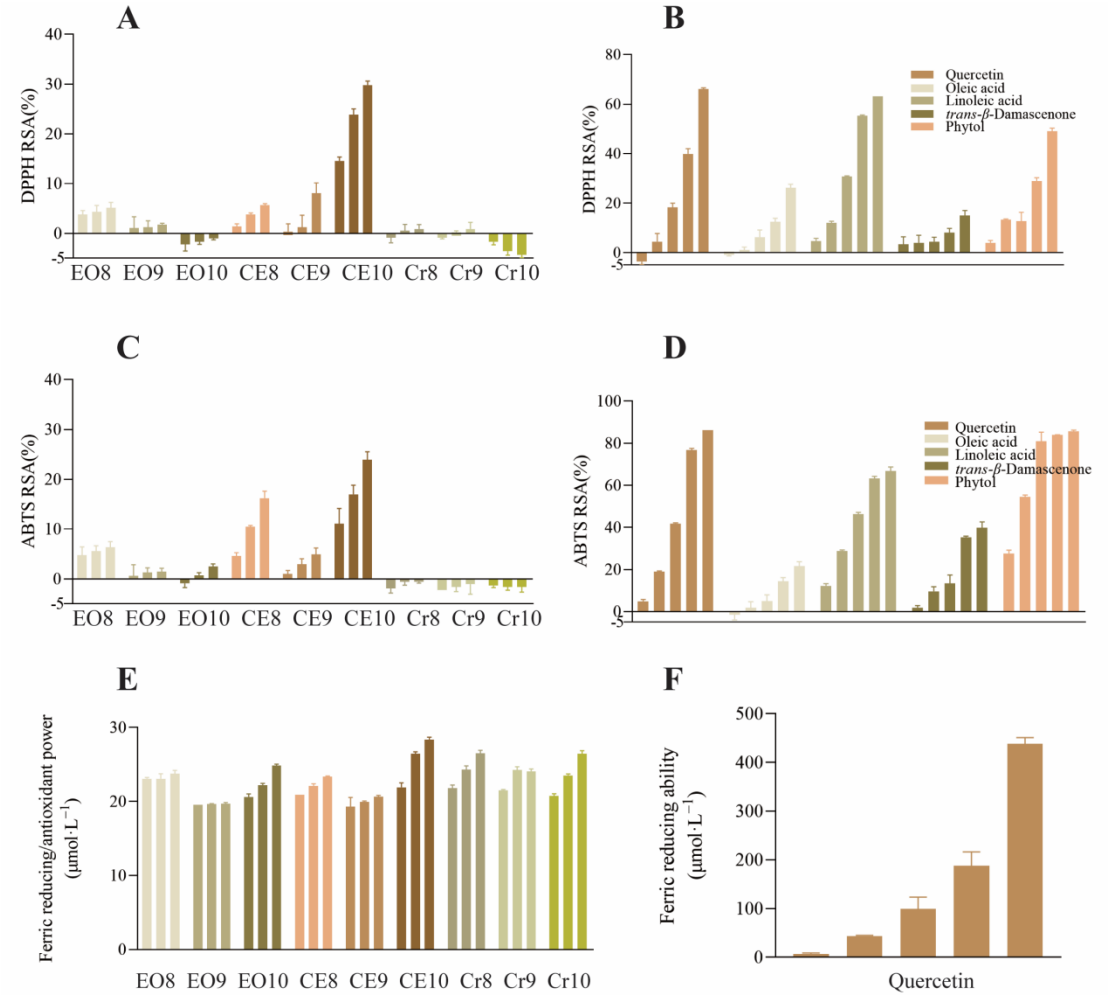

Figure 6. Antioxidant activity evaluation of *P. rotata* volatile oils and its constituents. A, C, E: Comparative analysis of RSA (DPPH, ABTS) and FRAP across nine samples of EOs, CEs, Crs tested at 50, 80, 110 μg/mL; B, D, F: Dose-dependent antioxidant capacity of selected compounds: Quercetin (positive control; 2.5–50 μmol/L), Oleic acid (100–2000 mmol/L), Linoleic acid (100–2000 mmol/L), *trans*-*β*-Damascenone (6.25–100 mmol/L), Phytol (6.25–100 mmol/L).

Phytol, *trans*-*β*-damascenone, linoleic acid, and oleic acid show some antioxidant capacities, especially phytol. Linoleic acid presents stronger antioxidant activities compared with oleic acid.

In the FRAP assay, the Crs showed different results compared to DPPH and ABTS, indicating some iron-reducing ability. This is likely due to the precipitation of FAs in the FRAP working solution and may not reflect their true antioxidant activity. This observation is also evident in the detection of chemical marker. Among the eight chemical markers, only phytol caused the working solution to change from brown to blue, but still exhibited some turbidity. In contrast, the positive control, quercetin, displayed a gradient change to a blue color upon reaction with the working solution, and the solution remained clear without any turbidity. It should be noted that the FRAP assay has limitations in measuring the antioxidant activities of lipophilic compounds without the addition of solubilizing agents[35]. Additionally, the turbidity of the working solution may be due to the water-based solvent and high concentrations of the tested samples.

It is important to note that even slight variations in experimental procedures can lead to significant differences in the obtained results for DPPH, ABTS, and FRAP assays. The outcomes of these assays are highly influenced by various factors[35].

It is worth noting that palmitic acid can induce oxidative stress, inflammation, insulin resistance, and impair endothelial function in a concentration-dependent manner[36,37]. Myristic acid can significantly stimulate human polymorphonuclear leukocytes, which play a crucial role in defending against microbial infections, to produce ROS. Excessive intake of myristic acid can lead to detrimental consequences due to uncontrolled ROS production[38].

Based on the results from DPPH, ABTS, and FRAP assays, three compounds such as phytol, *trans*-*β*-damascenone, and linoleic acid demonstrating superior antioxidant performance were selected for

further analysis. Their CAA were systematically evaluated using quercetin as the positive control (Fig. 7).

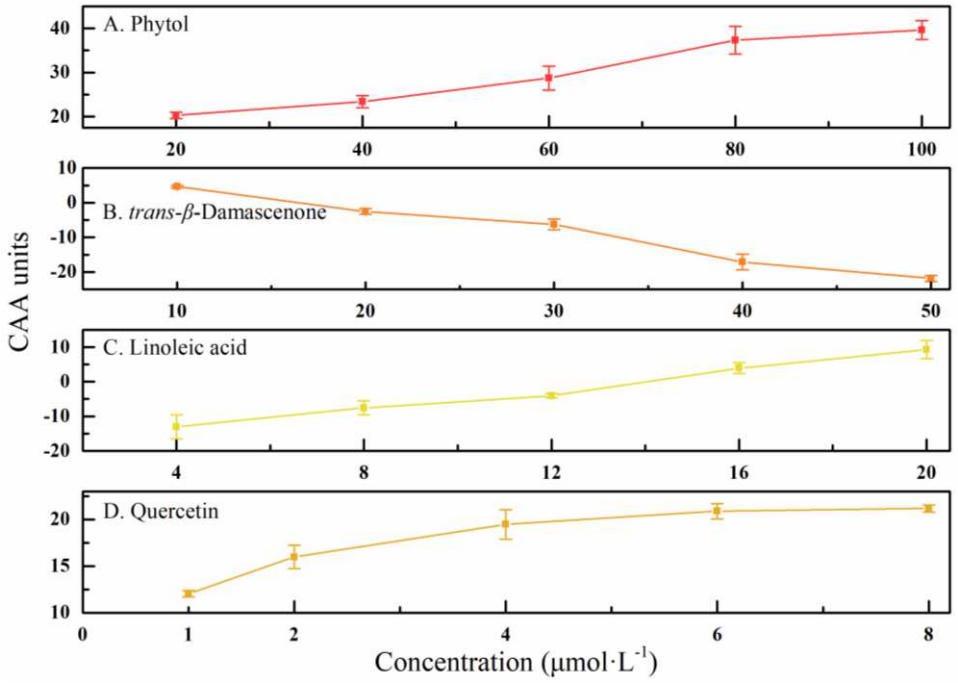

Figure 7. The CAA units of phytol, *trans*-*β*-damascenone and linoleic acid (quercetin as control).

CCK-8 assay-determined safe concentration ranges were established as follows: quercetin (1-8 μmol/L), *trans*-*β*-damascenone (10-50 μmol/L), linoleic acid (4-20 μmol/L), and phytol (20-100 μmol/L). Contrasting with chemical antioxidant assays, cellular-level evaluations revealed marked differences: linoleic acid exhibited significant activity only at higher concentrations (>15 μmol/L), while *trans*-*β*-damascenone demonstrated antioxidant effects at lower concentrations (<10 μmol/L) and progressively displayed pro-oxidative behavior at elevated doses (>10 μmol/L). Notably, phytol showed exceptional CAA performance with 40 μmol/L phytol exhibiting stronger antioxidant efficacy than 8 μmol/L quercetin.

Overall, among the EOs, Crs, and CEs, usually CEs present relatively strong antioxidant activities, particularly CE10. As for the eight chemicals, palmitic acid, myristic acid, methyl palmitate, and hexahydrofarnesyl acetone show no antioxidant capacities or pro-oxidant activities. On the other hand, oleic acid, linoleic acid, *trans*-*β*-damascenone, and phytol exhibit some antioxidant activities, especially phytol. In the CAA assay, the antioxidative activitiy of high concentration phytol was better than that of quercetin. The antioxidative activitiy of oleic acid, linoleic acid, and phytol are enhanced with increasing concentration, respectively.

Methyl palmitate can alleviate oxidative damage by inhibiting the production of malondialdehyde and increasing the enzyme activities of glutathione peroxidase, superoxide dismutase, and catalase. Its antioxidant activity has been validated in several *in vivo* models of chemical-induced toxicity[39]. However, this study found that methyl palmitate had no significant free radical scavenging activity or iron-reducing ability, suggesting that methyl palmitate primarily protects cells by enhancing the activity of endogenous antioxidants rather than directly scavenging ROS.

Oleic acid has been shown to prevent the production of ROS induced by palmitic acid in the endoplasmic reticulum[40]. Both oleic acid and linoleic acid are capable of exerting antioxidant activities by reducing pro-inflammatory signals[41]. Interestingly, linoleic acid exhibits better antioxidant capacities compared to oleic acid in the higher concentration group, which may be attributed to the differences of number and conjugation of double bonds present in linoleic acid and oleic acid[42,43]. Generally, polyunsaturated FAs with more double bonds and conjugations tend to exhibit better antioxidant activities[42,43], as the ROS have a tendency to react with the loosely bound electrons of the carbon double bonds, which are abundant in the fatty acyl chains of cell membrane lipid bilayers[44].

For phytol, the hydroxyl group can scavenge free radicals, and the double bonds contribute to the resonance structure that stabilizes free radicals[45]. Leaf EOs of *Celtis zenkeri* Engl., mainly composed of phytol, exhibited RSA equivalent to the same concentration of vitamin C and butylated hydroxyanisole in the DPPH assay[46]. On the other hand, phytol showed antibacterial effects by inducing oxidative stress in *Pseudomonas aeruginosa*[47]. Hexahydrofarnesyl acetone, as oxidation products of phytol, did not exhibit significant *in vitro* antioxidant capacity, consistent with the findings of Nazlić *et al.*[48].

Notably, several samples demonstrated higher RSA in the ABTS assay compared to the DPPH assay. This discrepancy likely arises from the enhanced reactivity of $ABTS^{\cdot+}$ radicals relative to the DPPH radical[49].

The CAA assay advances conventional chemical methods by incorporating cellular uptake, metabolism, and subcellular dynamics of antioxidants[25]. This system enhances translational value by evaluating antioxidant behavior within biological matrices, surpassing chemical assays focused solely on redox potential. Notably, these compounds exhibit distinct structural features—phytol contains alcoholic hydroxyl groups and double bond, *trans*-*β*-damascenone possesses ketone carbonyl moieties, and linoleic acid features double bonds—providing a comprehensive platform to investigate structure-activity relationships between functional groups and antioxidant efficacy. Notably, linoleic acid exhibited antioxidant activity exclusively at concentrations (≥15 μmol/L), though excessive linoleic acid intake (>400 μmol/L) has been associated with oxidative stress induction in rat skeletal muscle myoblasts[50]. Phytol had no obvious cytotoxicity when it was less than 100 μmol/L, which was better than quercetin (8 μmol/L) from 40-100 μmol/L. Phytol has been shown to increase the antioxidant enzyme activity in fish liver and inhibit lipid peroxidation[51]. This suggests that phytol has the potential to be a new antioxidant.

Conclusions

A total of 125 compounds are identified and quantified, of which 94 are reported for the first time from the EOs of *P. rotata*. In summary, 11 compounds, including palmitic acid, myristic acid, linoleic acid, oleic acid, methyl palmitate, hexahydrofarnesyl acetone, phytol, *trans*-*β*-damascenone, geraniol, linalool, and *α*-terpineol, are selected as the chemical markers, which are biosynthesized through FAs and MEP/DoXP pathways. Generally, CEs demonstrate stronger antioxidant capacities compared to EOs and Crs, which is likely influenced by the varying content of palmitic acid in these samples. Specifically, the percentage of palmitic acid, the most abundant compound, is found to be higher in Crs but lower in CEs compared to EOs. *In vitro* experiments demonstrate that oleic acid, linoleic acid, *trans*-*β*-damascenone, and phytol show some level of antioxidant activities, with phytol demonstrating the highest potency.

In future, we should investigate the synergistic effects of saturated FAs and monounsaturated FAs/polyunsaturated FAs and focus on chemicals that exhibit stronger antioxidant activities. The findings provide a foundation for future research on the biological activities and potential therapeutic uses of *P. rotata* EOs, emphasizing the need for *in vivo* studies to validate *in vitro* results and explore practical applications in medicine and industry.

Data availability

The dataset "The percentage of compounds in essential oils of *Phlomoides rotata* (Benth. ex Hook. f.) Mathiesen" is currently stored in the Springer Nature figshare repository with DOI: https://figshare.com/s/653dde388d6f4406113d.

Author Contributions: Conceptualization, Z.P. and J.W.; methodology, C.X. J.L., and J.W.; software, C.X., J.L., X.Y., and J.W.; validation, Z.P., C.X., J.L., X.Y., Y.S., and J.W.; investigation, C.X. and J.W.; resources, Z.P. and J.W.; data curation, C.X., J.L., X.Y. and J.W.; writing—original draft preparation, C.X., J.L., X.Y. and J.W.; writing—review and editing, Z.P., C.X., W.Z., X.Y., Y.S., A.H., N.K., S.A., M.E., and J.W.; supervision, Z.P. and J.W.; project administration, Z.P. and J.W.; funding acquisition, Z.P. and J.W. All authors have reviewed the manuscript.

Funding: This research project received funding from several sources, including the National Natural Science Foundation of China (Grant No. 81973567), the Chongqing Science and Technology Bureau and Chongqing Education Commission (Grant No. CSTB2023NSCQ-LZX0046), and the Chongqing Science and Technology Bureau (Grant No. cstc2020jcyj-msxmX0310).

Acknowledgments: The authors thank the undergraduates, Hang Shi, Qin Duan, Meiying Luo, Shanshan Jiang, and Churui Xiao, for their contributions.

Conflicts of Interest: The authors declare no conflict of interest.

References

1. Mathiesen, C., Scheen, A. C. & Lindqvist, C. Phylogeny and biogeography of the lamioid genus *Phlomis* (Lamiaceae). *Kew Bull.* **66**, 83–99 (2011).
2. The editorial board of Flora of China of Chinese Academy of Sciences. *Flora of China* (in Chinese, Volume 65 issue 2) 1, 480 (Science press, Beijing, China, 1977).
3. Li, H. & Hedge, I. C. *Flora of China* (*Lamiaceae*) (Volume 17) 50, 52, 156-157 (Science press, Beijing, China, 1994).
4. Pharmacopoeia committee of the People's Republic of China. *Pharmacopoeia of the People's Republic of China* (Volume I) 282 (China Medical Science and Technology Press, Beijing, China, 2025).
5. Nanjing University of Chinese medicine. *The dictionary of Chinese materia medica* (Volume 2) - 2nd edition 2390-2391 (Shanghai scientific and technical publishers, China, 2006).
6. Cui, Z. H. *et al.* Traditional uses, phytochemistry, pharmacology and toxicology of *Lamiophlomis rotata* (Benth.) Kudo: a review. *RSC Adv.* **10**, 11463 (2020).

7. Li, Y. *et al.* Lamiophlomis herba: A comprehensive overview of its chemical constituents, pharmacology, clinical applications, and quality control. *Biomed. Pharmacother.* **144**, 112299 (2021).
8. Schwab, W., Davidovich-Rikanati, R. & Lewinsohn, E. Biosynthesis of plant-derived flavor compounds. *Plant J.* **54**, 712-732 (2008).
9. Zhang, F. *et al.* Iridoid glucosides and a C_{13}-norisoprenoid from *Lamiophlomis rotata* and their effects on NF-kB activation. *Bioorg. Med. Chem. Lett.* **22**, 4447-4452 (2012).
10. Yin, X. F. Studies on the chemical constituents of *Lamiophlomis rotata* (dissertation). South-central University for Nationalities, Wuhan, China, 2015.
11. Liu, J. *et al.* Chemical variation in lipophilic composition of *Lamiophlomis rotata* from the Qinghai-Tibetan plateau. *Chem. Nat. Compd.* **42**, 525-528 (2006).
12. Liu, H. F., Li, X., Deng, Y., Song, X., & Li, H. Study on the chemical constituents of the essential oil from *Lamiophlomis rotata*. *Chin. J. Pharm. Anal.* **26**, 1794-1796 (2006).
13. Zhou, Z. *et al. Lamiophlomis rotata* attenuates rheumatoid arthritis by regulating sphingolipid and steroid hormone metabolism. *Mol. Omics* **19**, 72-83 (2023).
14. Aebisher, D., Cichonski, J., Szpyrka, E., Masjonis, S. & Chrzanowski, G. Essential oils of seven Lamiaceae plants and their antioxidant capacity. *Molecules* **26**, 3793 (2021).
15. Wang, J. *et al. Lamiophlomis rotata* identifification via ITS2 barcode and quality evaluation by UPLC-QTOF-MS couple with multivariate analyses. *Molecules* **23**, 3289 (2018).
16. Geng, X. *et al*. Total iridoid glycoside extract of *Lamiophlomis rotata* (Benth) *Kudo* accelerates diabetic wound healing by the NRF2/COX2 axis. *Chin. Med.* **19**, 53 (2024).
17. Yang, C. *et al*. Transcriptomic and proteomic investigation of the ameliorative effect of total polyphenolic glycoside extract on hepatic fibrosis in *Lamiophlomis rotata Kudo* via the AGE/RAGE pathway. *J. Ethnopharmacol.* **324**, 117720 (2024).
18. Van Den Dool, H. & Kratz, P. D. A generalization of the retention index system including linear temperature programmed gas-liquid partition chromatography. *J. Chromatogr.* **11**, 463-471 (1963).
19. Adams, R.P. *Identification of essential oil components by gas chromatography/mass spectrometry*, ed. 4.1. 1-804 (Allured publishing, Illinois, America, 2017).
20. Flavornet by Terry Acree & Heinrich Arn. https://www.flavornet.org/info/3033-23-6.html (2025).
21. Park, M. K., Cha, J. Y., Kang, M.-C., Jang, H. W., Choi, Y.-S. The effects of different extraction methods on essential oils from orange and tangor: From the peel to the essential oil. *Food Sci. Nutr.* **12**: 804–814 (2024).
22. Zengin, G. *et al. Crepis foetida* L. subsp. *rhoeadifolia* (Bieb.) Celak. as a source of multifunctional agents: Cytotoxic and phytochemical evaluation. *J. Funct. Foods* **17**, 698-708 (2015).
23. Re, R. *et al.* Antioxidant activity applying an improved ABTS radical cation decolorization assay. *Free Radical Bio. Med.* **26**, 1231-1237 (1999).
24. Liu, W. *et al.* Comparison of the effects of monounsaturated fatty acids and polyunsaturated fatty acids on liver lipid disorders in obese mice. *Nutrients* **15**, 3200 (2023).
25. Wolfe, K. L, & Liu, R. H. Cellular antioxidant activity (CAA) assay for assessing antioxidants, foods, and dietary supplements. *J. Agric. Food Chem.* **55**, 8896-8907 (2007).
26. Usami, A., Kashima, Y., Marumoto, S. & Miyazawa, M. Characterization of aroma-active compounds in dry flower of *Malva sylvestris* L. by GC-MS-O analysis and OAV calculations. *J. Oleo Sci.* **62**, 563-570 (2013).
27. Choi, H. S. GC-MS analyses of the essential oils from *Ixeris dentate* (Thunb.) Nakai and *I. stolonifera* A. Gray. *Korean J. Food Nutr.* **25**, 274-283 (2012).
28. Choi, H. S. Chemical composition of *Cirsium japonicum* var. *ussurience* Kitamura and the quantitative changes of major compounds by the harvesting season. *Korean J. Food Nutr.* **29**, 327-334 (2016).
29. Wang, J. Alkanes and chemical markers identified in the essential oil from pericarp of Nanfengmiju (*Citrus kinokuni* Hort. ex Tanaka). *J. Mex. Chem. Soc.* **67**, 82-93 (2023).
30. Carlin, S., Mattivi, F., Durantini, V., Dalledonne, S. & Arapitsas, P. Flint glass bottles cause white wine aroma identity degradation. *Proc. Nati. Acad. Sci.* **119**, e2121940119 (2022).
31. Pickenhagen, W. *Flavor Chemistry-Thirty Years of Progress* (ed. Teranishi, R., Wick, E. L. & Hornstein, I.) 75-87 (Kluwer Academic/Plenum Publishers, New York, U.S.A, 1999).
32. Kaneshima, T. *et al.* Isolation and identification of progenitors, glycoconjugates of *β*-damascenone precursors, in sweet potato (*Ipomoea batatas*). *Flavour Fragr. J.* **38**, 152-162 (2023).
33. Suzuki, M. *et al.* Identification of (3*S*, 9*R*)- and (3*S*, 9*S*)-megastigma-6,7-dien-3,5,9-triol 9-*O*-*β*-D-glucopyranosides as damascenone progenitors in the flowers of *Rosa damascena* Mill. *Biosci. Biotechnol. Biochem.* **66**, 2692-2697 (2002).
34. Dudareva, N., Klempien, A., Muhlemann, J. K. & Kaplan, I. Biosynthesis, function and metabolic engineering of plant volatile organic compounds. *New Phytol.* **198**, 16-32 (2013).
35. Munteanu, I. G. & Apetrei, C. Analytical methods used in determining antioxidant activity: A review. *Int. J. Mol. Sci.* **22**, 3380 (2021).
36. Fratantonio, D. *et al.* Palmitate-induced endothelial dysfunction is attenuated by cyanidin-3-*o*-glucoside through modulation of Nrf2/Bach1 and NF-κB pathways. *Toxicol Lett* **239**, 152–160 (2015).
37. Giorgio, M. *et al.* Electron transfer between cytochrome c and $p66^{shc}$ generates reactive oxygen species that trigger mitochondrial apoptosis. *Cell* **122**, 221–233 (2005).
38. Tada, M. *et al.* Myristic acid, a side chain of phorbol myristate acetate (PMA), can activate human polymorphonuclear leukocytes to produce oxygen radicals more potently than PMA. *J. Clin. Biochem. Nutr.* **45**, 309–314 (2009).
39. Hamed, A. B., Mantawy, E. M., El-Bakly, W. M., Abdel-Mottaleb, Y. & Azab, S. S. Methyl palmitate: the naturally occurring cardioprotective agent. *Arch. Pharm. Sci. Ain Shams Univ.* **4**, 47-62 (2020).
40. Sun, Y. *et al.* Oleic acid and eicosapentaenoic acid reverse palmitic acid-induced insulin resistance in human Hepg2 cells via the reactive oxygen species/*Jun* pathway. *Genom. Proteom. Bioinf.* **19**, 754–771 (2021).

41. Pauls, S. D. *et al.* Anti-inflammatory effects of *α*-linolenic acid in M1-like macrophages are associated with enhanced production of oxylipins from α-linolenic and linoleic acid. *J. Nutr. Biochem.* **57**, 121–129 (2018).
42. Wu, S. H. *et al.* Chemical composition analysis and antioxidant activity of essential oil from *Magnolia sieboldii* Leaves. *Mol. Plant Breed.* **21**, 1–12 (2023).
43. Lee, S. H. & Min, D. B. Effects, quenching mechanisms, and kinetics of carotenoids in chlorophyll-sensitized photooxidation of soybean oil. *J. Agri. Food Chem.* **38**, 1630–1634 (1990).
44. Hart, C. M., Tolson, J. K. & Block, E. R. Fatty acid supplementation protects pulmonary artery endothelial cells from oxidant injury. *Am. J. Respir. Cell Mol. BioI.* **3**, 479-489 (1990).
45. Islam, M. T. *et al.* Phytol: A review of biomedical activities. *Food Chem. Toxicol.* **121**, 82-94 (2018).
46. Okpala, E. O., Onocha, P. A. & Ali, M. S. Antioxidant activity of phytol dominated stem bark and leaf essential oils of *Celtis zenkeri* Engl.. *Trends Phytochem. Res.* **6**, 137-144 (2022).
47. Lee, W., Woo, E. R. & Lee, D. G. Phytol has antibacterial property by inducing oxidative stress response in *Pseudomonas aeruginosa*. *Free Radical Res.* **50**, 1309-1318 (2016).
48. Nazlić, M. *et al.* Endemic *Veronica saturejoides* Vis. ssp. *Saturejoides*-chemical composition and antioxidant activity of free volatile compounds. *Plants* **9**, 1646 (2020).
49. Teow, C. C. *et al.* Antioxidant activities, phenolic and *β*-carotene contents of sweet potato genotypes with varying flesh colours. *Food Chem.* **103**, 829-838 (2007).
50. Cao, X. *et al*. Excessive linoleic acid induces muscle oxidative stress through 5-lipoxygenase-dependent peroxidation. *Redox Biol.* **71**, 103096 (2024).
51. Ahani, S. *et al*. Effects of dietary phytol supplementation on growth performance, immunological parameters, intestinal bacteria, and prevention of oxidative stress following transportation of Nile Tilapia, *Oreochromis niloticus*. *Aq. Nutr.* **2024**, 7039179 (2024).

Figure 1. The chromatograms of EO10. Each denoted compound is assigned the corresponding code as listed in Table 1. "**A**" and "**B**" was obtained by GC-FID using a DB-5 column and GC-MS using a FFAP column, respectively.
Figure 2. The hypothetical transformation process from 5*β*, 6*α*-dihydroxy-3*β*-(*β*-D-glucopyranosyloxy)-7-megastigmen-9-one **(1)** to eight different types of C13-norisoprenoids. The arrows represent the enzymatic steps involved.
Figure 3. A Nineteen compounds were selected based on a VIP value of 1.2 or higher. **B** The PLS-DA scores plot. The nine samples were divided into three categories. **C** The loadings plot of each constituent in PLS-DA. The red-highlighted compounds demonstrate the most substantial contributions to both principal components 1 and 2, including: E14 (methyl margarate), CA4 (hexanoic acid), E11 (methyl hexadec-9-enoate), CA18 (stearic acid), CA15 (palmitic acid), MA13 (*cis*-geraniol), MA15 (geraniol), MA3 (linalool), N3 (*trans*-*β*-damascenone), N7 (*trans*-geranylacetone), Al18 (hexacosane), Al21 (nonacosane).
Figure 4. The main metabolic pathways. The color of the nodes is rendered based on the *p*-value (significance). The red circles usually represent a smaller *p*-value (high significance), indicating that the metabolite is differentially expressed or significantly enriched in the pathway. The size of the circles reflects the topological importance of the metabolite in the pathway, which is calculated based on topological parameters in the pathway analysis, such as node degree, betweenness centrality, *etc.*. The larger the circle, the stronger the connectivity of the metabolite in the pathway network, the more crucial its function, and the higher its overall impact (Impact Score) on the pathway. The color (significance) and size (importance) need to be analyzed in combination: nodes with high significance (red) and large circles are usually the key differentially expressed metabolites in the pathway and require special attention.
Figure 5. The biosynthesis of chemical markers. Solid arrows represent established biosynthetic steps, whereas dashed line arrows indicate the transformation is hypothetical. DMAPP, IPP, GGPP, and acp correspond to dimethylallyl diphosphate, isopentenyl diphosphate, geranylgeranyl diphosphate, and acyl-carrier protein, respectively.
Figure 6. Antioxidant activity evaluation of *P. rotata* volatile oils and its constituents. A, C, E: Comparative analysis of RSA (DPPH, ABTS) and FRAP across nine samples of EOs, CEs, Crs tested at 50, 80, 110 μg/mL; B, D, F: Dose-dependent antioxidant capacity of selected compounds: Quercetin (positive control; 2.5–50 μmol/L), Oleic acid (100–2000 mmol/L), Linoleic acid (100–2000 mmol/L), *trans*-*β*-Damascenone (6.25–100 mmol/L), Phytol (6.25–100 mmol/L).
Figure 7. The CAA units of phytol, linoleic acid, *trans*-*β*-damascenone and quercetin.

Supplementary Files

This is a list of supplementary files associated with this preprint. Click to download.

- SupplementalTable.docx